Cell. Mol. Life Sci. (2011) 68:125–137
DOI 10.1007/s00018-010-0446-z

Cellular and Molecular Life Sciences

RESEARCH ARTICLE

HCN2 channels in local inhibitory interneurons constrain LTP in the hippocampal direct perforant path

Lucas Matt · Stylianos Michalakis · Franz Hofmann · Verena Hammelmann · Andreas Ludwig · Martin Biel · Thomas Kleppisch

Received: 19 March 2010 / Revised: 21 June 2010 / Accepted: 23 June 2010 / Published online: 10 July 2010

Abstract Neuronal hyperpolarization-activated cyclic nucleotide-gated (HCN) channels are known to modulate spontaneous activity, resting membrane potential, input resistance, afterpotential, rebound activity, and dendritic integration. To evaluate the role of HCN2 for hippocampal synaptic plasticity, we recorded long-term potentiation (LTP) in the direct perforant path (PP) to CA1 pyramidal cells. LTP was enhanced in mice carrying a global deletion of the channel ($HCN2^{-/-}$) but not in a pyramidal neuron-restricted knockout. This precludes an influence of HCN2 located in postsynaptic pyramidal neurons. Additionally, the selective HCN blocker zatebradine reduced the activity of oriens-lacunosum moleculare interneurons in wild-type but not $HCN2^{-/-}$ mice and decreased the frequency of spontaneous inhibitory currents in postsynaptic CA1 pyramidal cells. Finally, we found amplified LTP in the PP of mice carrying an interneuron-specific deletion of HCN2. We conclude that HCN2 channels in inhibitory interneurons modulate synaptic plasticity in the PP by facilitating the GABAergic output onto pyramidal neurons.

Keywords Hippocampus · Long-term potentiation · Oriens-lacunosum moleculare interneurons · Perforant path · HCN channel

Abbreviations

HCN	Hyperpolarization-activated cyclic nucleotide-gated channels
LTP	Long-term potentiation
O-LM	Oriens-lacunosum moleculare interneuron
PP	Direct perforant pathway
SC	Schaffer collateral pathway

Electronic supplementary material The online version of this article (doi:10.1007/s00018-010-0446-z) contains supplementary material, which is available to authorized users.

L. Matt · F. Hofmann · T. Kleppisch (✉)
Institut für Pharmakologie und Toxikologie der Technischen Universität München, Biedersteiner Straße 29, 80802 Munich, Germany
e-mail: kleppisch@ipt.med.tum.de

L. Matt
e-mail: matt@ipt.med.tum.de

F. Hofmann
e-mail: hofmann@lrz.tum.de

S. Michalakis · V. Hammelmann · M. Biel
Department of Pharmacy, Center for Drug Research, Ludwig-Maximilians-Universität München, Butenandtstr. 7, 81377 Munich, Germany
e-mail: stylianos.michalakis@cup.uni-muenchen.de

V. Hammelmann
e-mail: verena.hammelmann@cup.uni-muenchen.de

M. Biel
e-mail: martin.biel@cup.uni-muenchen.de

A. Ludwig
Institut für Experimentelle und Klinische Pharmakologie und Toxikologie, Friedrich-Alexander-Universität Erlangen-Nürnberg, Fahrstr. 17, 91054 Erlangen, Germany
e-mail: ludwig@pharmakologie.uni-erlangen.de

F. Hofmann
DFG Forschergruppe 932, Munich, Germany

S. Michalakis · F. Hofmann · V. Hammelmann · M. Biel
Munich Center for Integrated Protein Science CIPSM, Butenandtstr. 7, 81377 Munich, Germany

Introduction

Hippocampal CA1 pyramidal neurons receive excitatory inputs to proximal dendrites via the Schaffer collaterals (SC) from CA3 pyramidal cells and the direct perforant path (PP, or temporoammonic input) projecting from layer III of the entorhinal cortex to their distal dendrites.

Voltage-gated channels influence dendritic integration of excitatory postsynaptic potentials in pyramidal cells (for review, see [1, 2]). Accordingly, Nolan et al. [3] provided compelling evidence for the behavioral role of I_h-dependent tuning of dendritic integration [4, 5]. HCN1 channels are highly expressed in the distal dendrites of CA1 pyramidal neurons. Consequently, HCN1 null mutants show selectively enhanced LTP in the PP input paralleled by improved spatial learning [3] likely due to attenuation of postsynaptic excitatory potentials at the distal dendrites. In vivo, hippocampal behavioral functions and synaptic plasticity additionally rely on local inhibition not examined in previous studies. A heterogeneous population of local inhibitory interneurons targeting CA1 pyramidal cells can (1) mediate feedback or feedforward inhibition, (2) set the threshold for initiation of axonal action potentials as well as dendritic Ca^{2+} spikes, and (3) participate in the generation of oscillatory activity [6–9]. Interestingly, several types of hippocampal inhibitory interneurons express I_h currents [10–14]. It was also reported that I_h currents inhibit pyramidal cells by facilitating spontaneous GABA release from stratum oriens interneurons [10], for example oriens-lacunosum moleculare (O-LM) cells [15]. This type of interneuron receives glutamatergic input from CA1 pyramidal cells and projects into the stratum lacunosum moleculare matching the site of PP inputs (for review, see [6, 15–18]).

Four subtypes (HCN1–4) of the hyperpolarization-activated cyclic nucleotide-gated channels (HCN) give rise to depolarizing I_h currents (for review, see [19]). The HCN1 and the HCN2 isoforms prevail in CA1 pyramidal neurons [20–22]. All four subtypes have been detected in GABAergic interneurons [11, 22], but details on their expression in O-LM interneurons remain unclear.

In this study, we show that LTP in the PP inputs to CA1 pyramidal cells is enhanced in the null mutant but not in a pyramidal neuron-specific conditional knockout of the HCN2 gene. Additionally, we observe increased LTP in an interneuron-specific knockout. Our work provides evidence that the HCN2 channel influences LTP in the direct perforant input to CA1 pyramidal cells through a function in inhibitory interneurons.

Materials and methods

Animals

Generation and breeding strategies of $HCN2^{-/-}$ [20] and $HCN1^{-/-}$ [23] mouse lines have been previously described. A mouse line carrying an HCN2 allele with two loxP sites flanking the exons 2 and 3 (L2 allele; Cre recombinase-mediated excision of which results in a frame shift) was crossed with either the Nex-Cre or the Dlx5/6-Cre mouse [24] to generate a conditional knockout lacking HCN2 in hippocampal pyramidal or inhibitory neurons, respectively. Accordingly, the conditional knockout animals (genotype: $HCN2^{L1/L2}$; $NEX^{+/Cre}$, $HCN2^{L1/L2}$; $DLX^{+/Cre}$) and the corresponding controls (genotype: $HCN2^{+/L2}$; $NEX^{+/Cre}$, $HCN2^{+/L2}$; $DLX^{+/Cre}$) are referred to as $HCN2^{PyrKO}$ or $HCN2^{InhKO}$ and $HCN2^{PyrCtr}$ or $HCN2^{InhCtr}$, respectively. Crossing $HCN2^{-/-}$ and $HCN1^{-/-}$ mice yielded double mutants (HCN-DKO) lacking both the HCN1 and the HCN2 subunit. Littermate offspring were used as control for all mutant mouse lines examined. All procedures were conducted in accordance to the German animal protection laws and the guidelines of the Deutsche Forschungsgemeinschaft.

Electrophysiology

Field EPSP recordings in hippocampal slices

Field EPSP recordings in hippocampal slices (fEPSP) were recorded as previously described [25]. Briefly, transverse hippocampal slices (400 µm thick) were prepared from 8- to 12-week-old mice using an egg-slicer [26] and then kept for ≥1.5 h in artificial cerebrospinal fluid (aCSF; 30°C; pH 7.4; in mM: 10 glucose, 3 KCl, 124 NaCl, 26 $NaHCO_3$, 1.25 NaH_2PO_4, 2.5 $CaCl_2$, 2 $MgSO_4$) bubbled with carbogen (95% O_2, 5% CO_2) before transferring them into a submerged type recording chamber constantly perfused with aCSF. To record fEPSPs in the SC pathway, stimulating and recording electrodes were positioned within the stratum radiatum near the CA3 region and in the CA1 region, respectively. Postsynaptic responses of PP inputs were obtained by placing stimulating and recording electrodes in the distal region of the stratum lacunosum moleculare. In addition, the CA1 region was separated from the CA3 region by a cut to avoid indirect activation of CA1 pyramidal neurons via CA3 or dentate gyrus cells [27]. fEPSPs were recorded using aCSF-filled glass pipettes (~3 MΩ) and an Axoclamp 2B amplifier (Axon Instruments). Stimulation and data acquisition were controlled by PULSE software (HEKA) via an ITC-16 computer interface (Instrutech). Stimuli (100 µs) were

delivered through a concentric bipolar electrode. The same intensity was used during baseline recording and induction of LTP using 4 trains of 50 stimuli at 100 Hz separated by 10 s. When indicated, 50 μM picrotoxin was washed into the bath solution.

Whole-cell patch-clamp recording

Acute slices (200–300 μm) were prepared from 2-week-old mice using a vibration microtome (Leica) as outlined elsewhere [28]. For recording, brain slices were placed in a recording chamber perfused continuously with aCSF bubbled with carbogen at room temperature. Hippocampal interneurons and pyramidal cells were visually identified under an upright microscope with DIC contrast [29]. Patch pipettes (2–3.5 MΩ) were pulled from borosilicate glass capillaries. All patch-clamp recordings were made in the whole-cell configuration using an EPC-9 amplifier and the PULSE software (HEKA). Current-clamp recordings of the membrane potential and voltage-clamp recordings of I_h currents in O-LM cells were performed using an intracellular solution containing (in mM): 10 glucose, 10 HEPES, 95 K-gluconate, 20 K_3-citrate, 10 NaCl, 0.5 $CaCl_2$, 1 $MgCl_2$, 0.02 EGTA, 1 KATP, 0.5 Na_2GTP. The extracellular solution in these experiments consisted of aCSF, supplemented with zatebradine (50 μM) or CsCl (4 mM) where indicated. Glutamatergic transmission was inhibited by kynurenic acid (2 mM) to isolate spontaneous action potentials [12]. This form of intrinsic activity was recorded from a considerable fraction of O-LM cells in the absence and presence of zatebradine. I_h currents were recorded in cells held at −45 mV during 2 s voltage-clamp steps to hyperpolarizing test potentials of −45 mV to −125 mV followed by a final step to −125 mV, a potential causing nearly complete activation. Current fractions activating during hyperpolarization were fitted to the following function: $I_{act}(V) = G_{rel}\ \ (V - V_{rev})/(1 + \exp((V - V_{1/2})/k)$, where G_{rel} is a relative conductance, V the test potential, V_{rev} the reversal potential calculated using to the Goldmann–Hodgkin–Katz equation, $V_{1/2}$ the potential corresponding to the midpoint of activation, and k a slope factor. More accurate determination of the voltage-dependence of I_h current activation was obtained based on the amplitude of instant tail currents ($I_{tail}[V]$) elicited during the voltage-clamp step to −125 mV following individual test pulses. The instant tail current is maximal (I_{max}) following the test pulse to −125 mV (full activation during test pulse), and minimal (I_{min}) following the test pulse to −45 mV (no activation during preceding test pulse). The voltage-dependence of I_h current activation can be described by the following Boltzmann function: $(I_{tail}[V] - I_{min})/(I_{max} - I_{min}) = 1/(1 + \exp[(V - V_{1/2})/k])$.

Whole-cell voltage-clamp recordings using the EPC-9 amplifier were made from the soma of visually identified CA1 pyramidal neurons to measure spontaneous inhibitory postsynaptic currents (sIPSC). sIPCSs were isolated pharmacologically from other synaptic currents by supplementing the standard extracellular solution (aCSF) with 25 μM 6,7-dinitroquinoxaline-2,3-dione (DNQX) and 50 μM (2R)-amino-5-phosphonovaleric acid (AP-5). Patch pipettes were filled with an intracellular solution containing (in mM): 125 CsCl, 10 HEPES, 1 EGTA, 0.1 $CaCl_2$, 2 Mg_2ATP, 0.2 Na_2GTP. The Cl^- reversal potential under these conditions was about 0 mV, and CA1 pyramidal neurons were held at −70 mV. Routinely, picrotoxin (50 μM) was added at the end of these experiments to confirm that synaptic currents were GABAergic.

Immunohistochemistry

Coronal brain slices (12 μm thick) from 8- to 12-week-old mice were fixed (5 min, 4% paraformaldehyde in phosphate buffered saline, PBS), and blocked/permeabilized for 2 h with 5% normal goat serum (NGS), 2% BSA and 0.3% Triton X-100 in PBS. The slices were then incubated overnight with the corresponding primary antibody (in 1% BSA/PBS). Endogenous peroxidase activity was quenched (3% H_2O_2 in PBS) for 10 min before sections were incubated with the corresponding secondary antibody. Primary antibodies used were: rabbit anti-HCN2 (1:500, Alomone), rabbit anti-HCN1 (1:500; Alomone), rat anti-somatostatin (1:100; Millipore). Secondary antibodies used to for detection were: peroxidase-conjugated donkey anti-rabbit (1:1,000; Jackson Immunoresearch) in combination with cyanine 3 tyramide signal amplification (TSA) kit (PerkinElmer), FITC-conjugated donkey anti-rat (1:100; Jackson Immunoresearch). After 10 min incubation with Hoechst 33342 (Invitrogen) sections were mounted with aqueous mounting medium (PermaFluor, Beckman-Coulter) and analyzed using an LSM 510 Meta confocal laser scanning microscope (Zeiss).

Western blot analysis

Brains from 8-week-old mice were removed. Hippocampus, olfactory bulb, thalamus and cortex were isolated. The individual tissue samples were homogenized at 900*g* (Potter S; B. Braun Biotech International) in cell lysis buffer (50 mM Tris–HCl pH 7.4, 150 mM NaCl, 1 mM EDTA, 1% Triton X-100) and centrifuged (14,000*g*, 4°C, 15 min). The protein concentration in the supernatant was determined by Bradford Assay. Subsequent SDS gel electrophoresis was performed with 80 μg protein per lane. After blotting, protein was immunodetected using a

polyclonal rabbit anti-HCN2 antibody (1:1,000, AB5378; Chemicon International). As a loading control, the blot was probed with an antibody against ATPase (1:500, clone α6F; developed by D.M. Fambrough, obtained from the Developmental Studies Hybridoma Bank, Iowa).

Data analysis

All data are represented as mean ± SEM. All LTP experiments show the slope of an averaged postsynaptic response. Routinely, four consecutive fEPSPs (corresponding to 1 min) were averaged. For statistical analysis of LTP, the average values during the last 5 min of the hour following tetanus were compared using Student's *t* test. Analysis of patch-clamp data was performed using PULSE/PULSEFIT (HEKA) and Origin 6.1 (OriginLab) including custom routines. Spontaneous spiking activity and spontaneous IPSCs were analyzed using MiniAnalysis package (version 6.0.9; Synaptosoft).

Results

Deletion of the HCN2 channel from principal neurons of the forebrain

Mice with a global [20] and a conditional deletion of the HCN2 gene in principal neurons of the forebrain were used to assess the role of the HCN2 channel subunit on hippocampal synaptic plasticity. Mice carrying loxP-flanked exons 2 and 3 of the HCN2 gene (L2 allele, Electronic supplementary material, ESM, Fig. 1a) were crossed with Nex-Cre mice expressing Cre recombinase under the control of the NEX gene promoter [24]. Within the telencephalon, activity of the NEX promoter marks glutamatergic principal neurons and is absent from GABAergic interneurons and macroglial cells [30]. This was reflected by effective recombination of the conditional L2 allele into the HCN2 knockout allele (L1) in hippocampal tissue of cells of the conditional knockout mouse observed with PCR and western blot analysis (ESM, Fig. 1b, c). In line with this, immunoreactivity for the HCN2 channel was virtually absent in the hippocampus of sections from the conditional knockout mice (Fig. 1a). Acknowledging the ablation of the HCN2 gene in pyramidal cells, we refer to the conditional knockout as $HCN2^{PyrKO}$ (genotype: $HCN2^{L1/L2}$; $NEX^{+/Cre}$) and to the corresponding controls as $HCN2^{PyrCtr}$ (genotype: $HCN2^{+/L2}$; $NEX^{+/Cre}$).

$HCN2^{PyrKO}$ mice do not display the CNS phenotypes observed in HCN2 null mutants [20] and have a normal life expectancy (data not shown). Both mouse lines lack gross anatomical abnormalities in the brain, and cellular layers in the hippocampus are regularly arranged.

HCN2 null mutants show enhanced LTP in direct PP inputs

A previous study demonstrated that mice bearing a knockout of the HCN1 channel in principal neurons of the forebrain show improved learning in a water maze [3]. This phenotype was thought to reflect changes in synaptic plasticity, namely elevated LTP in PP inputs to CA1 pyramidal cells. Using immunohistochemical stainings (Fig. 1a), we could confirm that, similar to HCN1, the HCN2 subunit is most extensively expressed in a small band corresponding to the stratum lacunosum moleculare [3, 22]. The resemblance of the hippocampal expression patterns of both the HCN1 and the HCN2 channels led to the speculation that HCN2 might serve a similar function in hippocampal synaptic plasticity as the HCN1 channel.

To establish the experimental conditions, we reproduced the phenotype of enhanced LTP in the PP input of HCN1 knockout mice without using a $GABA_A$ antagonist (ESM, Fig. 2). Using the same settings, we subsequently recorded LTP in global HCN2 knockout mice ($HCN2^{-/-}$). Resembling the findings for HCN1-deficient mice, $HCN2^{-/-}$ mice and the corresponding controls ($HCN2^{+/+}$) showed the same amount of LTP in the SC pathway (Fig. 1b), while there was a significant increase ($p < 0.01$) of LTP in the PP of mice lacking the HCN2 channel ($HCN2^{-/-}$: 167 ± 7%, $n = 6$ vs $HCN2^{+/+}$: 131 ± 6%, $n = 11$).

Mice lacking the HCN2 channel in glutamatergic cortical neurons show normal LTP in direct PP inputs

So far, these findings are in line with the idea that HCN2 channels serve a similar function for hippocampal synaptic plasticity as HCN1. To further strengthen this view, we additionally analyzed hippocampal LTP in $HCN2^{PyrKO}$ mice that have the HCN2 gene deleted in CA1 pyramidal neurons. As anticipated, LTP in the SC pathway (Fig. 1c, left panel) was not different between these mice and their controls ($HCN2^{PyrCtr}$: 135 ± 4%, $n = 18$ vs $HCN2^{PyrKO}$: 130 ± 4%, $n = 19$). However, to our surprise and in contrast to mice with a forebrain-specific lack of the HCN1 channel [3], $HCN2^{PyrKO}$ mice showed no increased LTP in the PP (Fig. 1c, right panel). We observed virtually the same amount of LTP in inputs to the distal dendrites of CA1 pyramidal cells in $HCN2^{PyrCtr}$ (132 ± 7%, $n = 9$) and $HCN2^{PyrKO}$ (127 ± 4%, $n = 13$) mice. Alterations in the basic properties of synaptic transmissions were excluded as source for these results in either $HCN2^{-/-}$ or $HCN2^{PyrKO}$ mice (ESM, Fig. 3).

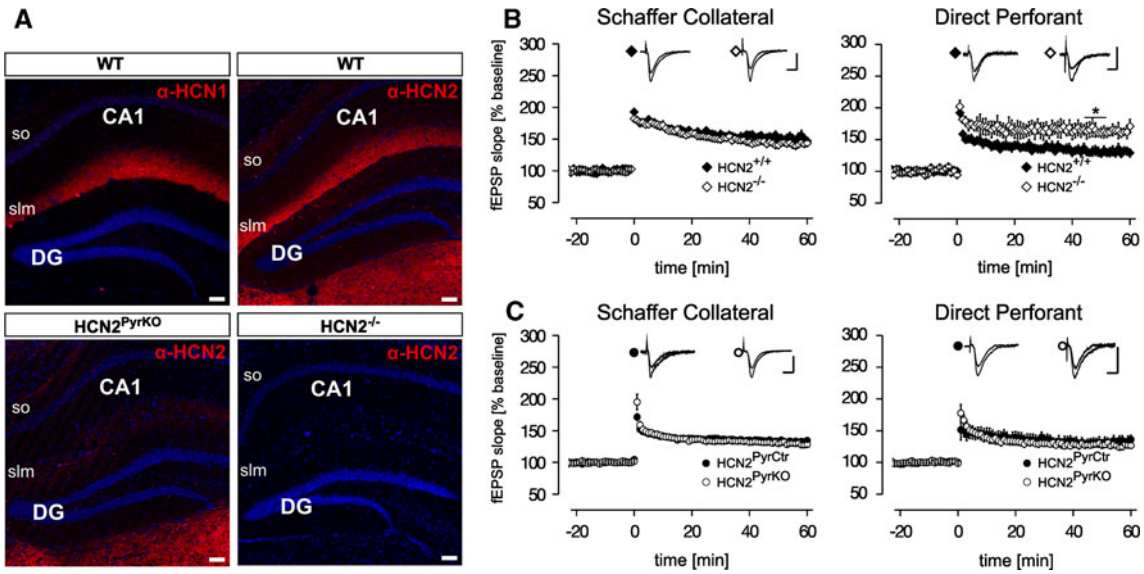

Fig. 1 Modulation of LTP in the PP does not depend on HCN2 expressed in postsynaptic pyramidal cells. **a** Immunohistochemical fluorescence labeling (*red*) in coronal brain sections of the wild-type (*WT*), the conditional HCN2 knockout ($HCN2^{PyrKO}$) and the HCN2 null mutation ($HCN2^{-/-}$) using specific antibodies against the HCN1 (α-HCN1) and the HCN2 (α-HCN2) channel. The ribbon-like distribution of the HCN2 channel protein in the hippocampus of the WT resembles that of the HCN1 channel with highest expression in the stratum lacunosum-moleculare (*slm*) corresponding to the distal dendrites of pyramidal cells. High levels of HCN2 immunoreactivity were also detected in thalamic areas ventral to the dentate gyrus (*DG*). Notice the substantial loss of the HCN2 protein in the *slm* of $HCN2^{PyrKO}$ revealing residual puncta-shaped immunoreactivity in various hippocampal layers including the stratum oriens (*so*). Sections from $HCN2^{-/-}$ mice completely lack immunoreactivity proving the specificity of the HCN2 antibody. *Scale bar* 100 µm. **b**,**c** Long-term potentiation (*LTP*) in Schaffer collateral (*SC*, *left panels*) and PP (*right panels*) of hippocampal slices from mutant mice lacking the HCN2 channel. Enhanced LTP was observed in the PP of HCN2 null mutants ($HCN2^{-/-}$), but not in the conditional knockout mice lacking HCN2 in pyramidal neurons ($HCN2^{PyrKO}$). *Scale bars* 10 ms, 1 mV. **b** LTP in $HCN2^{+/+}$ [*filled diamonds*; $n = 13/11$ (SC/PP)] and littermate $HCN2^{-/-}$ mice [*open diamonds*; $n = 16/6$ (SC/PP)]. **c** LTP in $HCN2^{PyrKO}$ [*open circles*; $n = 18/9$ (SC/PP)] and their littermate controls [$HCN2^{PyrCtr}$, *filled circles*; $n = 19/13$ (SC/PP)]. $^*p < 0.05$

$HCN2^{PyrKO}$ express HCN2 in local stratum oriens GABAergic interneurons

The absence of altered LTP in $HCN2^{PyrKO}$ mice may result from insufficient recombination in CA1 pyramidal cells of this mouse model. This possibility can be ruled out based on western blot data (ESM, Fig. 1). Additionally, there was a massive reduction of immunoreactivity in the hippocampus of $HCN2^{PyrKO}$ mice (Fig. 1a). While HCN2 immunoreactivity was completely absent in slices from $HCN2^{-/-}$ mice, weak residual staining was still present in the hippocampus of the $HCN2^{PyrKO}$ mice (Fig. 1a). This finding, together with the fact that the Nex-Cre mouse used to generate $HCN2^{PyrKO}$ mice lacks Cre expression in GABAergic interneurons [30], implies that $HCN2^{PyrKO}$ mice would lack the phenotype observed in HCN2 null mutants if it resulted primarily from a function of HCN2 channels in hippocampal inhibitory interneurons [18]. Accordingly, we hypothesized that the HCN2 channel facilitates output from local interneurons onto distal dendrites of CA1 pyramidal neurons. To test this hypothesis, we performed double immunostainings for the HCN2 channel and the neuropeptide somatostatin, a marker for oriens-lacunosum moleculare (O-LM) interneurons [31, 32] that are exemplary for the numerous types of dendrite-targeting interneurons [6]. HCN2 immunoreactivity was detected in the soma of somatostatin-positive cells in the stratum oriens of wild-type (WT) animals (Fig. 2a). Importantly, we observed the same coexpression in the stratum oriens of $HCN2^{PyrKO}$ animals (Fig. 2b) reinforcing the view that local interneurons in these mutants still express the HCN2 channel. Although HCN1 mRNA was previously reported in stratum oriens interneurons [21], we could not detect HCN1 immunoreactivity in the soma of any hippocampal interneuron (data not shown).

Inhibition of CA1 pyramidal cells is impaired in $HCN2^{-/-}$ mice

According to these findings, increased LTP in the PP of HCN2 null mutants may reflect a function of HCN2 channels driving inhibitory output from local interneurons onto distal dendrites of CA1 pyramidal neurons. In other words, a loss of these channels in the corresponding interneurons impairs inhibition of CA1 pyramidal cells.

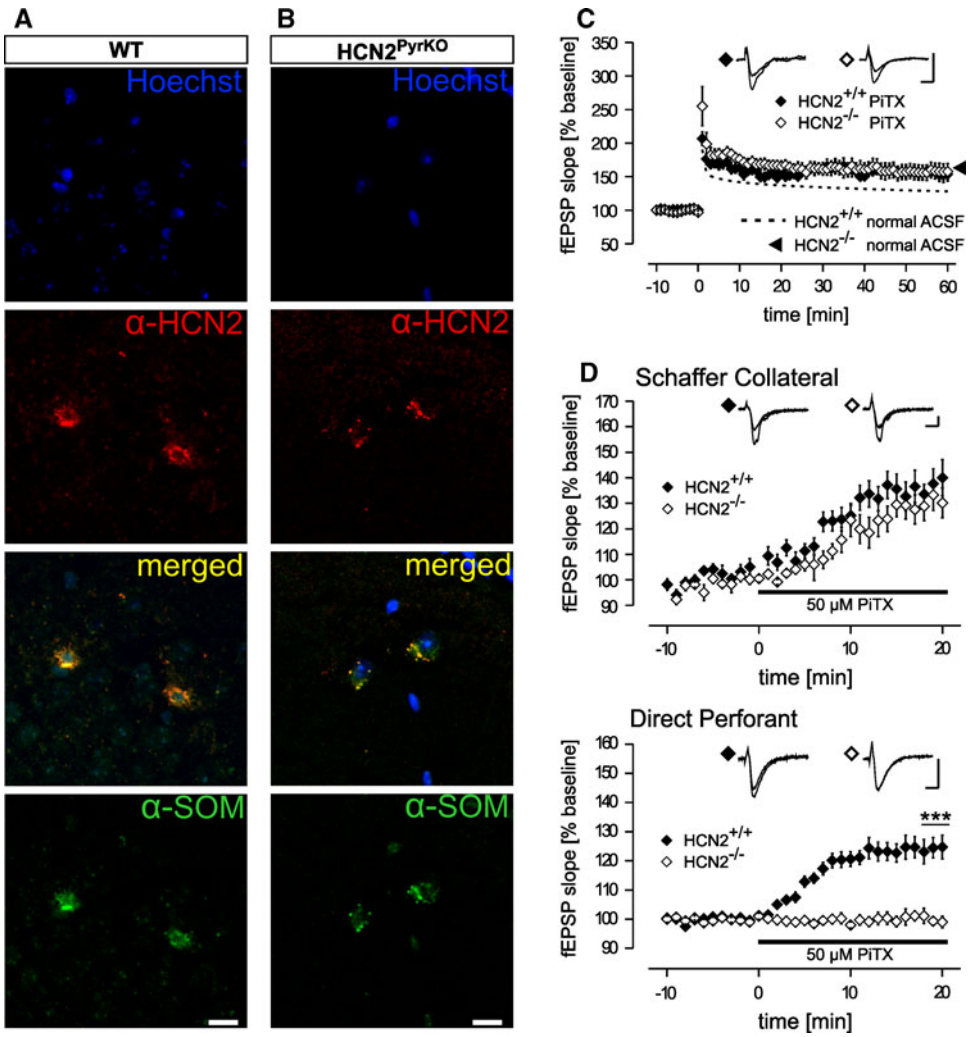

Fig. 2 The HCN2 channel is critical for the inhibition of synaptic transmission in the direct PP. **a**,**b** High magnification confocal fluorescent images of interneurons in the *so* of wild-type (WT) and $HCN2^{PyrKO}$ mice. In both genotypes, immunohistochemical labeling of the HCN2 channel (*red*) was found in the somata of interneurons in the *so* that were co-labeled by an antibody against somatostatin (α-SOM, *green*). Overlapping expression (*yellow*) is illustrated by merged images. Nuclei were counterstained using the nuclear marker Hoechst (*blue*). Individual experiments were reproduced with tissue from at least three different animals. *Scale bar* 10 µm. **c** WT ($HCN2^{+/+}$, *filled diamonds*, $n = 8$) mice and littermate HCN2 null mutants ($HCN2^{-/-}$, *open diamonds*, $n = 6$) show equivalent LTP in the direct PP under conditions of dysinhibition. The $GABA_A$ receptor-antagonist picrotoxin (PiTX, 50 µM) was present in all experiments. LTP in the absence of PiTX is indicated by the *dotted line* ($HCN2^{+/+}$) and the *arrowhead* ($HCN2^{-/-}$). *Scale bars* 10 ms, 1 mV. **d** Time course of the basal synaptic transmission in the SC pathway (*upper panel*) and PP (*lower panel*). The baseline level of synaptic transmission was recorded for about 10 min in normal aCSF before PiTX was washed in resulting in a failure to enhance the fEPSP slope in the PP of $HCN2^{-/-}$ mice. *Scale bars* 10 ms, 10 mV. $^{***}p < 0.001$

Therefore, we examined the effect of dysinhibition on LTP in the PP of WT and $HCN2^{-/-}$ mice (Fig. 2c). Fitting with our assumption, the $GABA_A$ receptor-antagonist picrotoxin (PiTX, 50 µM) had no effect on LTP in the mutants ($HCN2^{-/-}$ with PiTX: 160 ± 12%, $n = 6$), but it increased LTP in PP inputs of the WT on average by about 25% ($HCN2^{+/+}$ with PiTX: 155 ± 9%, $n = 8$). In fact, block of $GABA_A$ receptor-mediated synaptic transmission abolished the difference in LTP between both genotypes seen with intact inhibition ($HCN2^{-/-}$ without PiTX: 167 ± 7%, $n = 6$ vs $HCN2^{+/+}$ without PiTX: 131 ± 6%, $n = 11$). We further tested for possible alterations in the inhibition of the basal synaptic transmission due to HCN2 gene deletion. Field EPSPs were evoked every 15 s in glutamatergic inputs to CA1 pyramidal cells of WT and $HCN2^{-/-}$ mice. Under basal conditions, the slope of the field EPSPs in both genotypes did not differ in either pathway. Following wash-in of picrotoxin, the slope of field EPSPs measured in the SC pathway showed a prominent increase in both genotypes (Fig. 2d). However, picrotoxin failed to increase the slope of field EPSPs measured in the PP of the $HCN2^{-/-}$ mice, while it did in

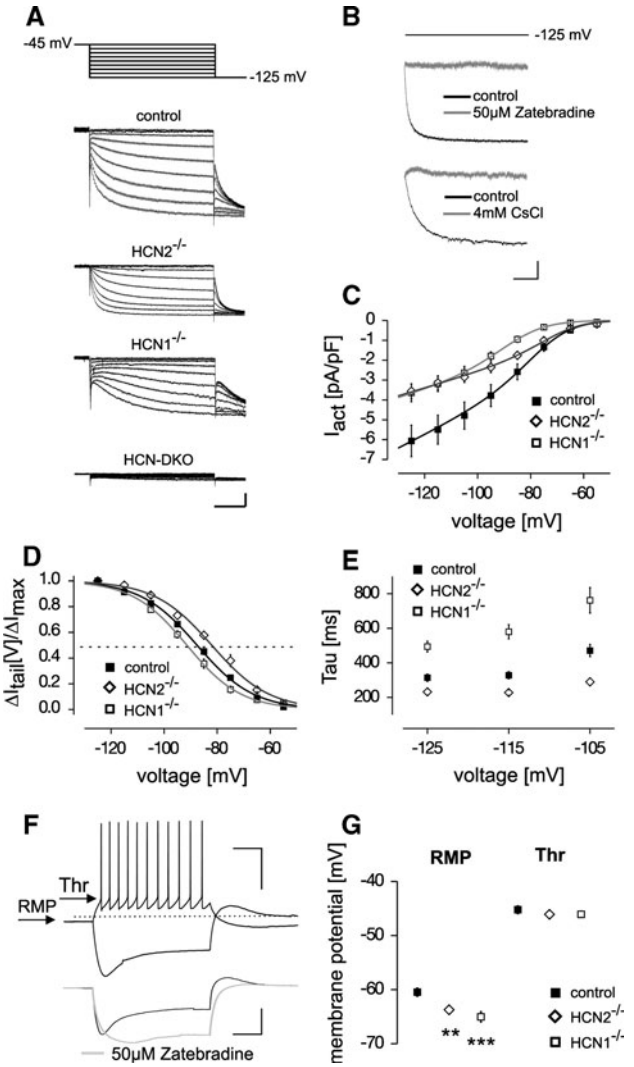

Fig. 3 HCN2 channels mediate a major portion of I_h currents in oriens-lacunosum moleculare (O-LM) interneurons and regulate the resting membrane potential (RMP). Whole-cell patch-clamp recordings were performed in O-LM cells of wild-type (WT) (*control*), HCN2$^{-/-}$ and HCN1$^{-/-}$ mice. **a** Representative whole-cell voltage-clamp recordings of I_h currents in O-LM cells (*lower panels*) of WT (*control*), HCN2$^{-/-}$ mice, HCN1$^{-/-}$ mice and double mutants (HCN-DKO) lacking both subunits. Currents were evoked by 2-s hyperpolarizing voltage-clamp steps applied from a holding potential of −45 mV in 10 mV increments and followed by a final voltage-clamp step to −125 mV (*top panel*). O-LM cells of HCN2$^{-/-}$ mice show decreased current density. Essentially no I_h currents were detected in HCN-DKO mice at physiological membrane potentials. *Scale bars* 500 ms and 200 pA. **b** Hyperpolarization-activated membrane currents in O-LM cells are sensitive to blockers of I_h currents. Currents were measured at −125 mV in the absence (*control*, *back traces*) and in the presence (*gray traces*) of cesium chloride (*Cs*, 4 mM) and zatebradine (50 µM). *Scale bars* 500 ms and 200 pA. **c** Voltage relationship of the slowly activating current (I_{act}) evoked by hyperpolarizing voltage-clamp steps normalized to cell capacity (instantaneous currents were not taken into account). Smooth curves represent the fit of I_{act} (see "Materials and methods"). On average, I_{act} at −125 mV was −6.0 ± 0.7 pA/pF (*control*, *filled squares*, $n = 35$), −3.3 ± 0.4 pA/pF (HCN2$^{-/-}$, *open diamonds*, $n = 20$, $p < 0.01$) and −3.6 ± 0.4 pA/pF (HCN1$^{-/-}$, *open squares*, $n = 22$, $p < 0.05$). **d** Voltage-dependence of the tail current elicited at −125 mV (for details, see "Materials and methods"). Midpoints of I_h current activation were estimated as −85.0 ± 0.7 mV (*control*, $n = 35$), −81.3 ± 1.3 mV (HCN2$^{-/-}$, $n = 20$, $p < 0.01$) and −90.4 ± 1.2 mV (HCN1$^{-/-}$, $n = 22$, $p < 0.001$). **e** Activation kinetics of I_h currents in O-LM cells estimated by a single exponential fit. At −125 mV I_h currents activated with a time constant of 314 ± 21 ms (*control*, $n = 35$), 232 ± 19 ms (HCN2$^{-/-}$, $n = 20$, $p < 0.05$) and 494 ± 31 ms (HCN1$^{-/-}$, $n = 22$, $p < 0.001$). **f** Typical response of O-LM cells from control animals to injection of depolarizing and hyperpolarizing current pulses, respectively. RMP was measured with zero current injected. Depolarization beyond a threshold potential (*Thr*) evoked a weakly accommodating train of action potentials followed by slow afterhyperpolarization. A prominent depolarizing voltage sag was present upon hyperpolarization which was completely blockable by zatebradine. *Scale bars* 500 ms and 50 mV. *Dotted line* −60 mV. **g** Mean values of the RMP and the threshold for action potential firing (*Thr*) in control ($n = 21$), HCN2$^{-/-}$ ($n = 21$) and HCN1$^{-/-}$ ($n = 24$) mice. $^{**}p < 0.01$, $^{***}p < 0.001$

WT littermates. Taken together, these data suggest a selective defect of inhibitory inputs to the distal dendrites of CA1 pyramidal cells under basal conditions and during high-frequency stimulation of the corresponding glutamatergic inputs.

HCN2 channels contribute to I_h currents and the resting membrane potential in oriens-lacunosum moleculare (O-LM) interneurons

To further verify our immunohistochemical data on a functional level, we performed whole-cell patch-clamp experiments on O-LM interneurons in the CA1 region. O-LM cells are thought to represent the major fraction of stratum oriens interneurons [15]. We identified O-LM cells by their location within the stratum oriens, their visual appearance and electrophysiological properties [6, 33, 34]. To assess the contribution of the HCN2 subunit to I_h currents in O-LM cells (Fig. 3a), we compared the density of I_h currents in HCN1$^{-/-}$ and HCN2$^{-/-}$ mice with that in the corresponding controls (HCN1$^{+/+}$ and HCN2$^{+/+}$). There was no difference between HCN1$^{+/+}$ and HCN2$^{+/+}$ mice in the capacity-corrected density of I_h currents allowing us to combine the data to a common control. These hyperpolarization-activated currents were sensitive to I_h blockers such as cesium and zatebradine as illustrated by recordings from WT animals (Fig. 3b). Under the experimental conditions used, O-LM cells in slices from HCN2$^{-/-}$ mice showed a decrease in I_h current density of about 50% compared to the control (Fig. 3c). In addition, the voltage-dependence of I_h activation in HCN1$^{-/-}$ mice is shifted towards more negative membrane potentials, while a shift towards more positive values was observed in HCN2$^{-/-}$. This suggested that the remaining I_h current in O-LM cells lacking the HCN2 channel is conducted by HCN1 channels activating at more

positive membrane potentials (Fig. 3d). Accordingly, the remaining I_h currents in HCN2$^{-/-}$ activated much faster than in the control, again reflecting the contrasting properties [35] of either the HCN1 or the HCN2 channel subunit (Fig. 3e).

Fitting well, the density of I_h currents in O-LM cells from HCN1$^{-/-}$ mice was also reduced by about 50%, and changes of activation kinetics mirrored those for HCN2$^{-/-}$ mice (Fig. 3a, c, e). Finally, O-LM cells in the compound knockout (genotype: HCN1$^{-/-}$; HCN2$^{-/-}$) showed virtually no residual I_h currents indicating that the expression of HCN3 and HCN4 subunits in these cells is negligible (Fig. 3a). Fits of the current–voltage relationships for the current fraction activating during hyperpolarizing voltage-clamp steps represented by the corresponding curves yielded relative conductances (G_{rel}; for details, see "Materials and methods") of 2.04 ± 0.02 nS ($n = 35$) for the control, 1.33 ± 0.11 nS ($n = 22$) for the HCN1$^{-/-}$ and 1.30 ± 0.15 nS ($n = 20$) for the HCN2$^{-/-}$ mice.

Current-clamp measurements in O-LM cells revealed a marked depolarizing voltage sag in response to injection of hyperpolarizing currents that was abolished by the selective blocker of I_h currents zatebradine (Fig. 3f). The lack of the HCN2 channel was reflected primarily by a negative shift of the membrane potential both at rest and with hyperpolarizing currents injected. Suggesting relevant HCN2 channel activity at normal resting membrane potential (RMP), O-LM cells from HCN2$^{-/-}$ mice (−63.2 ± 0.8 mV, $n = 21$) showed a significantly ($p < 0.01$) more hyperpolarized RMP than control cells (−60.7 ± 0.4 mV, $n = 32$) (Fig. 3g). A similar shift of the RMP in O-LM cells was observed for mice lacking the HCN1 channel (−65.1 ± 1.0 mV, $n = 27$). Unlike for the RMP, neither the deletion of the HCN2 nor the HCN1 gene had an effect on the threshold potential for repetitive spiking in O-LM cells (control: −43.1 ± 0.6 mV, 21; HCN2$^{-/-}$: −43.1 ± 0.9 mV, 21; HCN1$^{-/-}$: −43.8 ± 0.7 mV, $n = 24$).

Inhibition of CA1 pyramidal cells is impaired in HCN2$^{-/-}$ mice

Activity of local GABAergic interneurons can also be monitored indirectly by recording spontaneous inhibitory postsynaptic potentials (sIPSC) in CA1 pyramidal cells. Therefore, we analyzed the frequency and amplitude of sIPSCs measured in CA1 pyramidal cells from WT and HCN2$^{-/-}$ mice. Further supporting the view that the HCN2 channel is critical for the function of local interneurons, the frequency of sIPSCs (Fig. 4a) recorded in CA1 pyramidal cells of HCN2$^{-/-}$ mice (2.1 ± 0.2 Hz, $n = 6$) was significantly ($p < 0.05$) reduced compared to that in the control mice (4.0 ± 0.5 Hz, $n = 8$). Zatebradine, the selective blocker of I_h currents significantly ($p < 0.01$) reduced the frequency of sIPSCs in the latter to 1.7 ± 0.3 Hz ($n = 8$), a level similar to that observed in HCN2$^{-/-}$ mice under control conditions. The zatebradine-induced decrease of sIPSC frequency was less pronounced in the HCN2$^{-/-}$ mice (1.3 ± 0.1 Hz, $n = 6$). Genotype and zatebradine had no significant effect on the sIPSC amplitude (Fig. 4a). Picrotoxin completely abolished sIPSCs in all genotypes (Fig. 4a, upper panel).

Extending these experiments, we examined spontaneous activity (Fig. 4c) observed in a substantial part of O-LM cells with kynurenic acid present in the bath solution [12]. Strikingly, the HCN blocker zatebradine (50 μM) significantly ($p < 0.01$) reduced the frequency of spontaneous activity under these conditions selectively in the control mice ($\Delta F/F_{basal}$ 0.32 ± 0.05, $n = 12$) and had no effect in the HCN2$^{-/-}$ mice ($\Delta F/F_{basal}$ −0.04 ± 0.12, $n = 6$).

Complementary to a previous report [10], these findings indicate that spontaneous activity of local inhibitory interneurons targeting CA1 pyramidal cells critically depends on the function of HCN2 channels.

LTP is enhanced by the deletion of HCN2 from forebrain GABAergic neurons

To further evaluate the importance of HCN2-dependent inhibitory transmission for LTP in the PP, we additionally generated mice lacking HCN2 in forebrain GABAergic neurons using the Dlx5/6-Cre mouse [36]. Expression of Cre under control of the regulatory sequences of the Dlx5/Dlx6 genes leads to recombination of the HCN2 L2 allele in differentiating and migrating forebrain GABAergic neurons during embryonic development [37, 38]. Accordingly, the resulting conditional knockout is referred to as HCN2^{InhKO} (genotype: HCN2$^{L1/L2}$; DLX$^{+/Cre}$) while HCN2^{InhCtr} (genotype: HCN2$^{+/L2}$; DLX$^{+/Cre}$) are the corresponding controls. In contrast to HCN2$^{-/-}$ [20], HCN2^{InhKO} mice do not display any obvious CNS phenotypes and have a normal life expectancy (data not shown). We were not able to observe any abnormalities in the brain and the hippocampal cellular layers.

Successful Cre-mediated conditional deletion of the HCN2 gene was confirmed in inhibitory interneurons using whole-cell patch-clamp recordings. As expected, I_h currents in O-LM cells of HCN2^{InhKO} showed reduced amplitudes and accelerated activation kinetics (Fig. 5a, b). Especially, the voltage-dependence of I_h activation was shifted significantly to more positive membrane potentials (Fig. 5c). The remaining hyperpolarization-activated currents were still susceptible to inhibition by zatebradine (data not shown).

Supporting our hypothesis of the role of HCN2 channels in hippocampal inhibitory interneurons, LTP in the PP of brain slices from HCN2^{InhKO} mice (161 ± 7%, $n = 5$) was significantly ($p < 0.05$) enhanced (Fig. 5d) compared to

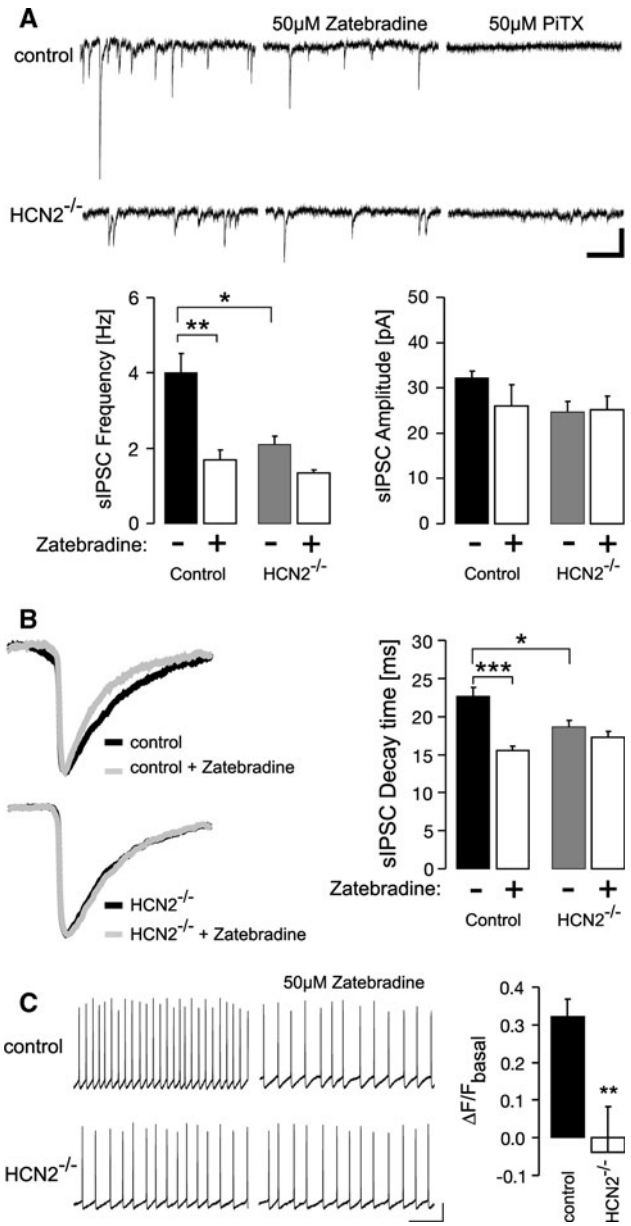

◀ **Fig. 4** The HCN2 channel supports spontaneous inhibitory postsynaptic currents (*sIPSCs*) in CA1 pyramdial cells and the spontaneous activity of oriens-lacunosum moleculare (O-LM) interneurons. Whole-cell patch-clamp recordings were performed in O-LM cells of wild-type (*control*) and HCN2$^{-/-}$ mice. **a** HCN2$^{-/-}$ mice show a reduced frequency of sIPSCs and reduced zatebradine-sensitivity compared to the control. *Upper panels* show representative voltage-clamp recordings of sIPSCs from CA1 pyramidal neurons of control and HCN2$^{-/-}$ mice under control conditions (*left*), in the presence of zatebradine (50 μM, *middle*) and picrotoxin (50 μM, *right*). *Lower panels* illustrate the mean sIPSC frequency (*left*) and amplitude (*right*) for both genotypes in the absence (−) and presence (+) of zatebradine. *Scale bar* 20 pA, 500 ms. **b** Averaged sIPSCs from control and HCN2$^{-/-}$ mice in the absence (*black*) and presence (*gray*) of zatebradine. The *bar diagram* illustrates the mean decay time of the sIPCSs for the corresponding genotype and conditions. Mean decay time in the control was 22.7 ± 1.2 ms ($n = 8$) and 15.5 ± 0.6 ms ($n = 8$) in the absence (−) and presence (+) of zatebradine, respectively. The corresponding mean decay time in the HCN2$^{-/-}$ mice was 18.6 ± 0.9 ms ($n = 6$) and 17.3 ± 0.7 ms ($n = 6$). **c** Effect of zatebradine on spontaneous spiking activity in O-LM cells from control and HCN2$^{-/-}$ mice with kynurenic acid (2 mM) present throughout the experiment. *Left panels* show representative recordings prior and after application of zatebradine. *Right panel* illustrates the mean decrease in spiking frequency ($\Delta F = F_{basal} - F_{zatebradine}$)) induced by the I_h channel blocker. All data were normalized to the basal frequency (F_{basal}) of spontaneous spiking prior to the application of zatebradine ($\Delta F/F_{basal}$). *Scale bars* 500 ms and 20 mV. *$p < 0.05$, **$p < 0.01$, ***$p < 0.001$

littermate HCN2^{InhCtr} (134 ± 3%, $n = 5$). Basal synaptic transmission was not affected in the PP of HCN2^{InhKO} mice (ESM, Fig. 4).

Discussion

The present study demonstrates for the first time a critical role of the HCN2 channel for the GABAergic output from hippocampal inhibitory interneurons and its functional impact on hippocampal synaptic plasticity.

Hippocampal expression of HCN2 channels and alterations of synaptic plasticity observed in HCN2$^{-/-}$ mice were similar to those reported for the HCN1 subtype, which constrains synaptic plasticity most effectively in the PP by damping excitatory postsynaptic potentials at the distal dendrites of CA1 pyramidal cells where it is maximally expressed [3]. Also, the HCN2 subunit is strongly expressed in the stratum lacunosum moleculare, where the distal dendrites of pyramidal cells receive glutamatergic inputs from the thalamus and the entorhinal cortex. Functionally reflecting this expression pattern, HCN2$^{-/-}$ exhibited increased LTP in the PP without alterations in the SC pathway projecting to the proximal dendrites of CA1 pyramidal cells. However, we observed normal LTP the PP of mice carrying a pyramidal neuron-specific deletion of the HCN2 gene (HCN2^{PyrKO}). This proves that, in contrast to HCN1, HCN2 does not constrain LTP in PP inputs by modulating dendritic integration in pyramidal neurons.

Insufficient efficiency of the Cre/lox-mediated recombination is ruled out by our western blot and immunohistochemical data. Furthermore, the Nex promoter fragment used for Cre-mediated deletion of the HCN2 gene does not drive expression in inhibitory interneurons [30]. The distribution of residual immunoreactivity in the hippocampus of HCN2^{PyrKO} mice matches that of local inhibitory interneurons [6, 18]. Therefore, we suggest that the HCN2-mediated constrainment of LTP in the PP is associated with a facilitatory function of this channel for inhibitory output from local interneurons to the distal dendrites of CA1 pyramidal cells. In this scenario, loss of

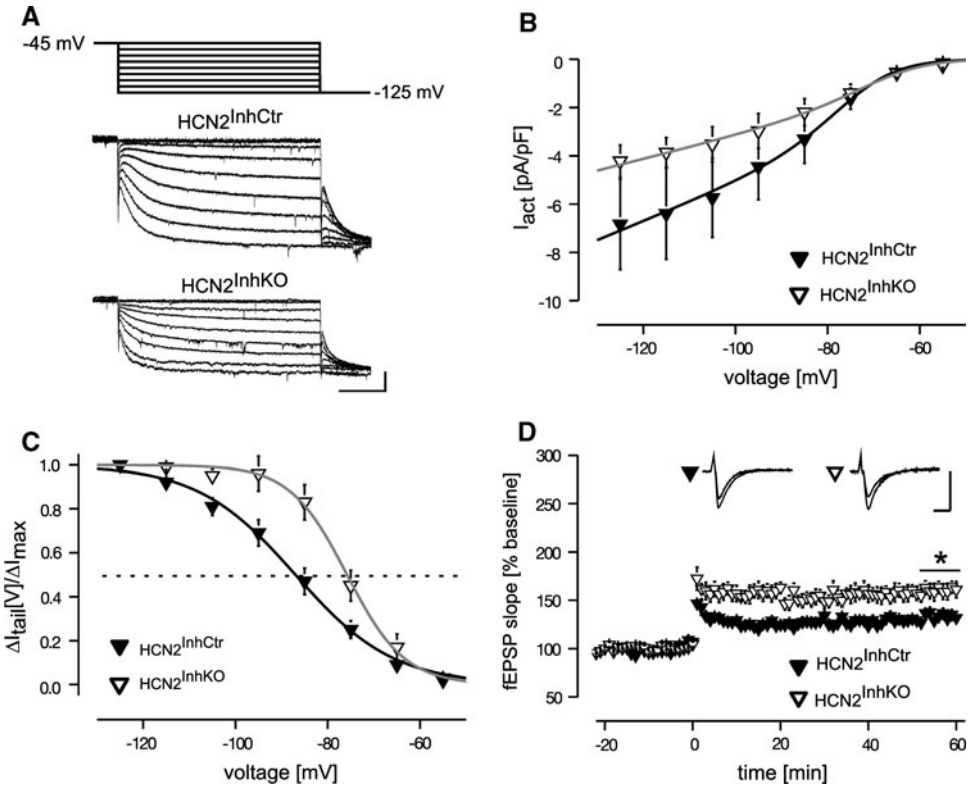

Fig. 5 LTP is enhanced in the PP of mice lacking the HCN2 channel in forebrain GABAergic neurons ($HCN2^{InhKO}$). **a** Representative whole-cell voltage-clamp recordings of I_h currents in O-LM cells (*lower panels*) of $HCN2^{InhCtr}$ and $HCN2^{InhKO}$ in response to 2-s hyperpolarizing voltage-clamp steps applied from a holding potential of −45 mV in 10 mV increments and followed by a final voltage-clamp step to −125 mV (*top panel*). **b** Voltage relationship of the slowly activating current (I_{act}) evoked by hyperpolarizing voltage-clamp steps normalized to cell capacity. Smooth curves represent the fit of I_{act}. On average, I_{act} at −125 mV was −6.8 ± 1.9 pA/pF ($HCN2^{InhCtr}$, *filled triangles*, $n = 6$) and −4.2 ± 0.7 pA/pF ($HCN2^{InhKO}$, *open triangles*, $n = 5$). **c** Voltage-dependence of the tail current elicited at −125 mV. Midpoints of I_h current activation were estimated as −84.9 ± 2.0 mV ($HCN2^{InhCtr}$, $n = 6$) and −75.6 ± 1.6 mV ($HCN2^{InhKO}$, $n = 5$, $p < 0.05$). **d** LTP is enhanced in the PP of $HCN2^{InhKO}$ (*open triangles*, $n = 5$) compared to littermate controls ($HCN2^{InhCtr}$, *filled triangles*, $n = 5$)

the HCN2 channel should induce dysinhibition in $HCN2^{-/-}$ mice. Fittingly, treatment with the $GABA_A$ receptor-antagonist picrotoxin had no effect on LTP in the PP path of these mice, while it increased LTP in control animals to the level observed in the mutants. Additionally, picrotoxin failed to strengthen basal synaptic transmission in the PP of $HCN2^{-/-}$ mice, while it did in the SC pathway. Basal synaptic transmission in the WT was picrotoxin-sensitive in both pathways. Providing further evidence for decreased activity of local GABAergic interneurons, the sIPSC frequency recorded in CA1 pyramidal neurons of $HCN2^{-/-}$ mice was significantly reduced compared with the WT. This finding is not related to compensatory changes induced by gene deletion, as the selective I_h blocker zatebradine virtually abolished the genotype-difference. Supplemental confirmation comes from the fact that LTP is enhanced in the PP of a mouse lacking HCN2 selectively in forebrain GABAergic neurons ($HCN2^{InhKO}$).

Hippocampal inhibitory interneurons represent a diverse cell population [6, 7]. Can we provide information regarding the type of interneuron(s) potentially involved in HCN2-mediated regulation of LTP in the PP? Several types of hippocampal interneurons express I_h currents [10–14], including oriens-lacunosum moleculare (O-LM) interneurons. Unique anatomical and electrophysiological features qualify this cell type as a supreme candidate to influence synaptic transmission in the PP. Located in the stratum oriens, they receive excitatory inputs from CA1 pyramidal cells and provide inhibitory feedback to their distal dendrites in the stratum lacunosum moleculare [16, 17, 39, 40]. Although the involvement of other interneuronal cell-types cannot be excluded, the following findings suggest that O-LM interneurons at least contribute to the HCN2-mediated suppression of LTP in the PP. In the somata of stratum oriens interneurons of both WT and $HCN2^{PyrKO}$ animals, we found colocalized immunoreactivity for HCN2 and somatostatin (Fig. 2a, b), a

neuropeptide expressed in O-LM cells [41–44]. In line with this, HCN2 channels contributed significantly to I_h currents recorded in O-LM cells, reflected by the hyperpolarized membrane potential found in HCN2$^{-/-}$ mice. Additionally, the I_h blocker zatebradine significantly reduced spontaneous spiking of O-LM cells in WT but not HCN2$^{-/-}$ mice. Together, these findings suggest that HCN2 channels strengthen the inhibitory output from O-LM interneurons. This function of the HCN2 channels in O-LM interneurons might be representative for the channel's function in other types of interneurons possibly involved in the inhibition of distal inputs to CA1 pyramidal cells. If HCN2 channels were regulating the function of interneurons projecting to proximal or perisomatic regions of CA1 pyramidal cells, LTP in the SC pathway were expected to be altered. Yet in our hands, HCN2 channels exclusively influenced synaptic plasticity in the PP, underscoring the functional impact of interneurons connected to distal dendrites of CA1 pyramidal cells. Alternatively, interneurons in the stratum lacunosum moleculare could exert feed-forward inhibition [cf. 45], but at least a subpopulation of these neurons is not involved as blocking I_h currents does not influence their intrinsic firing [13]. The potential function of I_h in stratum lacunosum moleculare interneurons remains to be elucidated. Additionally, non-uniform innervation of hippocampal pyramidal neurons should be considered. It is feasible that CA1 pyramidal cells densely targeted by PP afferents are mainly inhibited by O-LM cells.

How can impaired inhibitory activity boost synaptic plasticity in the PP? For instance, it may facilitate propagation of dendritic spikes in distal synapses, an effect possibly strengthened by cooperative activity of more proximal SC synapses (for review, see [1]). Furthermore, reduced GABAergic input in the stratum lacumosum moleculare allows back-propagation of action potentials [46, 47] to the apical tuft of pyramidal cells, resulting in the potentiation of synapses from the entorhinal cortex that are active during CA1 ripple oscillations in vivo and facilitate LTP in the corresponding inputs in vitro. O-LM interneurons, for example, provide an important portion of inhibition directed onto the distal dendrites of CA1 pyramidal cells in a feedback loop [16, 48, 49] and perhaps also due to spontaneous activity. These cells develop sustained inhibition proportional to the rate of incoming action potentials [40] thereby saturating inhibitory output to distal dendrites of CA1 pyramidal cells in response to their repetitive activation. Accordingly, decreased feedback inhibition during repetitive stimulation of PP afferents may account for the increased LTP in HCN2$^{-/-}$ mice. Others have shown that I_h currents support the spontaneous activity of O-LM cells [10, 12].

How do HCN2 channels strengthen the inhibitory output onto pyramidal cells generated by activation of O-LM or other interneurons? I_h modulates cellular properties including spontaneous activity, resting membrane potential, input resistance, afterpotential, rebound activity, and dendritic integration ([2], for review, see [19, 50]), functions that may strongly depend on the cellular localization of the HCN channels. Hyperpolarization of the resting membrane potential as observed in O-LM cells of HCN2-deficient mice is assumed to reduce excitability. Concurrently, elimination of the depolarizing conductance leads to enhanced excitability due to an increased input resistance. The latter effect predominates for dendritically expressed HCN channels. In contrast, somatically expressed HCN channels are thought to facilitate neuronal excitability. Our immunohistochemical findings indeed indicate somatic expression of the HCN2 channel in O-LM interneurons agreeing with the view that it supports the activity of these cells. Further, our data demonstrate that HCN1 channels are not located in the somata of O-LM cells and likely serve a different function in these cells. However, the current data does not indicate the intracellular location of HCN1 and HCN2 in other types of local hippocampal interneurons.

Presently, one can only speculate about the behavioral relevance of disinhibition-induced alterations in the synaptic plasticity of HCN2-deficient mice. There is compelling evidence that appropriate storage of spatial information in the hippocampus relies on PP inputs from the entorhinal cortex [51–53], thought to fine tune the representation of the environment by hippocampal place cells in the CA1 region. Recent findings in HCN1-deficient mice not only underline the function of the PP in spatial learning but also suggest a functional link to synaptic plasticity in this pathway [3]. Despite the fact that mechanisms underlying regulation of synaptic plasticity in CA1 pyramidal cells by HCN1 (modulates dendritic intergration in distal dendrites) and HCN2 (modulates inhibition of distal dendrites) channels apparently differ, one may predict a similar effect on hippocampus-dependent learning. Actually, there is convincing evidence regarding a functional link between activity of GABAergic interneurons, LTP and hippocampus-dependent learning. For example, in a mouse neurofibromatosis model, deficits in spatial learning are due to increased activity of GABAergic interneurons leading to decreased LTP [54, 55].

In conclusion, we suggest that HCN2 channels serve an important function in setting the activity of hippocampal inhibitory interneurons, and that HCN2 channel-dependent GABAergic output onto distal dendrites of CA1 pyramidal cells constrains LTP in the PP. Moreover, the HCN2 channel is expressed in and promotes the excitability of O-LM interneurons, a cell type qualified to mediate such type of regulation.

Acknowledgments The authors thank John L. Rubenstein and Marc Ekker for providing the Dlx5/6-Cre mouse line. This work was supported by a grant from the Deutsche Forschungsgemeinschaft to Thomas Kleppisch (KL1172/2-4).

References

1. Spruston N (2008) Pyramidal neurons: dendritic structure and synaptic integration. Nat Rev Neurosci 9:206–221
2. Magee JC (2000) Dendritic integration of excitatory synaptic input. Nat Rev Neurosci 1:181–190
3. Nolan MF, Malleret G, Dudman JT, Buhl DL, Santoro B, Gibbs E, Vronskaya S, Buzsaki G, Siegelbaum SA, Kandel ER, Morozov A (2004) A behavioral role for dendritic integration: HCN1 channels constrain spatial memory and plasticity at inputs to distal dendrites of CA1 pyramidal neurons. Cell 119:719–732
4. Magee JC (1998) Dendritic hyperpolarization-activated currents modify the integrative properties of hippocampal CA1 pyramidal neurons. J Neurosci 18:7613–7624
5. Magee JC (1999) Dendritic lh normalizes temporal summation in hippocampal CA1 neurons. Nat Neurosci 2:508–514
6. Klausberger T (2009) GABAergic interneurons targeting dendrites of pyramidal cells in the CA1 area of the hippocampus. Eur J Neurosci 30:947–957
7. Maccaferri G, Lacaille J-C (2003) Interneuron Diversity series: Hippocampal interneuron classifications–making things as simple as possible, not simpler. Trends Neurosci 26:564–571
8. Miles R, Toth K, Gulyas AI, Hajos N, Freund TF (1996) Differences between somatic and dendritic inhibition in the hippocampus. Neuron 16:815–823
9. Whittington MA, Traub RD (2003) Interneuron diversity series: inhibitory interneurons and network oscillations in vitro. Trends Neurosci 26:676–682
10. Lupica CR, Bell JA, Hoffman AF, Watson PL (2001) Contribution of the hyperpolarization-activated current (I(h)) to membrane potential and GABA release in hippocampal interneurons. J Neurophysiol 86:261–268
11. Aponte Y, Lien CC, Reisinger E, Jonas P (2006) Hyperpolarization-activated cation channels in fast-spiking interneurons of rat hippocampus. J Physiol 574:229–243
12. Maccaferri G, McBain CJ (1996) The hyperpolarization-activated current (Ih) and its contribution to pacemaker activity in rat CA1 hippocampal stratum oriens-alveus interneurones. J Physiol 497:119–130
13. Chapman CA, Lacaille JC (1999) Intrinsic theta-frequency membrane potential oscillations in hippocampal CA1 interneurons of stratum lacunosum-moleculare. J Neurophysiol 81:1296–1307
14. Ali AB, Thomson AM (1998) Facilitating pyramid to horizontal oriens-alveus interneurone inputs: dual intracellular recordings in slices of rat hippocampus. J Physiol 507:185–199
15. Maccaferri G (2005) Stratum oriens horizontal interneurone diversity and hippocampal network dynamics. J Physiol 562:73–80
16. Blasco-Ibanez JM, Freund TF (1995) Synaptic input of horizontal interneurons in stratum oriens of the hippocampal CA1 subfield: structural basis of feed-back activation. Eur J Neurosci 7:2170–2180
17. Katona I, Acsady L, Freund TF (1999) Postsynaptic targets of somatostatin-immunoreactive interneurons in the rat hippocampus. Neuroscience 88:37–55
18. Freund TF, Buzsaki G (1996) Interneurons of the hippocampus. Hippocampus 6:347–470
19. Biel M, Wahl-Schott C, Michalakis S, Zong X (2009) Hyperpolarization-activated cation channels: from genes to function. Physiol Rev 89:847–885
20. Ludwig A, Budde T, Stieber J, Moosmang S, Wahl C, Holthoff K, Langebartels A, Wotjak C, Munsch T, Zong X, Feil S, Feil R, Lancel M, Chien KR, Konnerth A, Pape HC, Biel M, Hofmann F (2003) Absence epilepsy and sinus dysrhythmia in mice lacking the pacemaker channel HCN2. EMBO J 22:216–224
21. Bender RA, Brewster A, Santoro B, Ludwig A, Hofmann F, Biel M, Baram TZ (2001) Differential and age-dependent expression of hyperpolarization-activated, cyclic nucleotide-gated cation channel isoforms 1–4 suggests evolving roles in the developing rat hippocampus. Neuroscience 106:689–698
22. Notomi T, Shigemoto R (2004) Immunohistochemical localization of Ih channel subunits, HCN1–4, in the rat brain. J Comp Neurol 471:241–276
23. Nolan MF, Malleret G, Lee KH, Gibbs E, Dudman JT, Santoro B, Yin D, Thompson RF, Siegelbaum SA, Kandel ER, Morozov A (2003) The hyperpolarization-activated HCN1 channel is important for motor learning and neuronal integration by cerebellar Purkinje cells. Cell 115:551–564
24. Schwab MH, Bartholomae A, Heimrich B, Feldmeyer D, Druffel-Augustin S, Goebbels S, Naya FJ, Zhao S, Frotscher M, Tsai MJ, Nave KA (2000) Neuronal basic helix-loop-helix proteins (NEX and BETA2/Neuro D) regulate terminal granule cell differentiation in the hippocampus. J Neurosci 20:3714–3724
25. Kleppisch T, Wolfsgruber W, Feil S, Allmann R, Wotjak CT, Goebbels S, Nave KA, Hofmann F, Feil R (2003) Hippocampal cGMP-dependent protein kinase I supports an age- and protein synthesis-dependent component of long-term potentiation but is not essential for spatial reference and contextual memory. J Neurosci 23:6005–6012
26. Katz LC (1987) Local circuitry of identified projection neurons in cat visual cortex brain slices. J Neurosci 7:1223–1249
27. Yeckel MF, Berger TW (1990) Feedforward excitation of the hippocampus by afferents from the entorhinal cortex: redefinition of the role of the trisynaptic pathway. Proc Natl Acad Sci USA 87:5832–5836
28. Lacinova L, Moosmang S, Langwieser N, Hofmann F, Kleppisch T (2008) Cav1.2 calcium channels modulate the spiking pattern of hippocampal pyramidal cells. Life Sci 82:41–49
29. Dodt HU, Zieglgansberger W (1990) Visualizing unstained neurons in living brain slices by infrared DIC-videomicroscopy. Brain Res 537:333–336
30. Goebbels S, Bormuth I, Bode U, Hermanson O, Schwab MH, Nave KA (2006) Genetic targeting of principal neurons in neocortex and hippocampus of NEX-Cre mice. Genesis 44:611–621
31. Somogyi P, Klausberger T (2005) Defined types of cortical interneurone structure space and spike timing in the hippocampus. J Physiol 562:9–26
32. Losonczy A, Zhang L, Shigemoto R, Somogyi P, Nusser Z (2002) Cell type dependence and variability in the short-term plasticity of EPSCs in identified mouse hippocampal interneurones. J Physiol 542:193–210
33. Minneci F, Janahmadi M, Migliore M, Dragicevic N, Avossa D, Cherubini E (2007) Signaling properties of stratum oriens interneurons in the hippocampus of transgenic mice expressing EGFP in a subset of somatostatin-containing cells. Hippocampus 17:538–553
34. Lawrence JJ, Statland JM, Grinspan ZM, McBain CJ (2006) Cell type-specific dependence of muscarinic signalling in mouse hippocampal stratum oriens interneurones. J Physiol 570:595–610
35. Baruscotti M, Bucchi A, Difrancesco D (2005) Physiology and pharmacology of the cardiac pacemaker (“funny”) current. Pharmacol Ther 107:59–79

36. Monory K, Massa F, Egertova M, Eder M, Blaudzun H, Westenbroek R, Kelsch W, Jacob W, Marsch R, Ekker M, Long J, Rubenstein JL, Goebbels S, Nave KA, During M, Klugmann M, Wolfel B, Dodt HU, Zieglgansberger W, Wotjak CT, Mackie K, Elphick MR, Marsicano G, Lutz B (2006) The endocannabinoid system controls key epileptogenic circuits in the hippocampus. Neuron 51:455–466
37. Zerucha T, Stuhmer T, Hatch G, Park BK, Long Q, Yu G, Gambarotta A, Schultz JR, Rubenstein JL, Ekker M (2000) A highly conserved enhancer in the Dlx5/Dlx6 intergenic region is the site of cross-regulatory interactions between Dlx genes in the embryonic forebrain. J Neurosci 20:709–721
38. Stuhmer T, Puelles L, Ekker M, Rubenstein JL (2002) Expression from a Dlx gene enhancer marks adult mouse cortical GABAergic neurons. Cereb Cortex 12:75–85
39. Mittmann W, Chadderton P, Hausser M (2004) Neuronal microcircuits: frequency-dependent flow of inhibition. Curr Biol 14:R837–R839
40. Pouille F, Scanziani M (2004) Routing of spike series by dynamic circuits in the hippocampus. Nature 429:717–723
41. Naus CC, Bloom FE (1988) Immunohistochemical analysis of the development of somatostatin in the reeler neocortex. Brain Res 471:61–68
42. Baude A, Nusser Z, Roberts JD, Mulvihill E, McIlhinney RA, Somogyi P (1993) The metabotropic glutamate receptor (mGluR1 alpha) is concentrated at perisynaptic membrane of neuronal subpopulations as detected by immunogold reaction. Neuron 11:771–787
43. Maccaferri G, Roberts JD, Szucs P, Cottingham CA, Somogyi P (2000) Cell surface domain specific postsynaptic currents evoked by identified GABAergic neurones in rat hippocampus in vitro. J Physiol 524:91–116
44. Klausberger T, Magill PJ, Marton LF, Roberts JD, Cobden PM, Buzsaki G, Somogyi P (2003) Brain-state- and cell-type-specific firing of hippocampal interneurons in vivo. Nature 421:844–848
45. Elfant D, Pal BZ, Emptage N, Capogna M (2008) Specific inhibitory synapses shift the balance from feedforward to feedback inhibition of hippocampal CA1 pyramidal cells. Eur J Neurosci 27:104–113
46. Markram H, Lubke J, Frotscher M, Sakmann B (1997) Regulation of synaptic efficacy by coincidence of postsynaptic APs and EPSPs. Science 275:213–215
47. Spruston N, Schiller Y, Stuart G, Sakmann B (1995) Activity-dependent action potential invasion and calcium influx into hippocampal CA1 dendrites. Science 268:297–300
48. Maccaferri G, McBain CJ (1995) Passive propagation of LTD to stratum oriens-alveus inhibitory neurons modulates the temporoammonic input to the hippocampal CA1 region. Neuron 15:137–145
49. Lacaille JC, Mueller AL, Kunkel DD, Schwartzkroin PA (1987) Local circuit interactions between oriens/alveus interneurons and CA1 pyramidal cells in hippocampal slices: electrophysiology and morphology. J Neurosci 7:1979–1993
50. Pape HC (1996) Queer current and pacemaker: the hyperpolarization-activated cation current in neurons. Annu Rev Physiol 58:299–327
51. Brun VH, Leutgeb S, Wu HQ, Schwarcz R, Witter MP, Moser EI, Moser MB (2008) Impaired spatial representation in CA1 after lesion of direct input from entorhinal cortex. Neuron 57:290–302
52. Brun VH, Otnass MK, Molden S, Steffenach HA, Witter MP, Moser MB, Moser EI (2002) Place cells and place recognition maintained by direct entorhinal-hippocampal circuitry. Science 296:2243–2246
53. Remondes M, Schuman EM (2004) Role for a cortical input to hippocampal area CA1 in the consolidation of a long-term memory. Nature 431:699–703
54. Cui Y, Costa RM, Murphy GG, Elgersma Y, Zhu Y, Gutmann DH, Parada LF, Mody I, Silva AJ (2008) Neurofibromin regulation of ERK signaling modulates GABA release and learning. Cell 135:549–560
55. Costa RM, Federov NB, Kogan JH, Murphy GG, Stern J, Ohno M, Kucherlapati R, Jacks T, Silva AJ (2002) Mechanism for the learning deficits in a mouse model of neurofibromatosis type 1. Nature 415:526–530